

Ab initio molecular dynamics simulations of the adsorption on complex surfaces

Axel Groß

Institut für Theoretische Chemie
Universität, 89081 Ulm, Germany
E-mail: axel.gross@uni-ulm.de

Ab initio molecular dynamics (AIMD) simulations represent a versatile tool to study dynamical processes of molecules, solids and/or surfaces as will be demonstrated focusing on the adsorption dynamics of molecules on nanostructured surfaces such as precovered or stepped surfaces. Performing AIMD simulations corresponds to unbiased computer experiments allowing the identification of mechanistic processes whose sequence is sometimes unexpected. This will be illustrated using the H₂ adsorption on a precovered surface without any dimer vacancies as an example. In addition, first results related to the adsorption of molecular oxygen on stepped platinum surfaces will be presented.

1 Introduction

In ab initio molecular dynamics simulations, the forces necessary to integrate the classical equations of motions are calculated *on the fly* using some suitable first-principles total-energy electronic structure method¹. This makes the method very versatile since no fitting of multi-dimensional potential energy surfaces is required which can be rather cumbersome². Yet, in particular for the adsorption dynamics on metal surfaces, such AIMD simulations have been prohibitively expensive just a few years ago allowing only the determination of a few trajectories^{3,4}. However, due to the development of efficient periodic electronic structure codes^{5,6} based on density functional theory (DFT) and the improvement in the available computer power this situation has now changed. It has become possible to determine thousands of trajectories of molecules impinging on surfaces⁷⁻⁹. Note that the statistical uncertainty of reaction probabilities does not depend on the complexity of the system making the determination of statistically significant reaction probabilities on structured surfaces possible.

Furthermore, the AIMD simulations provide an unbiased view on dynamical processes on surfaces. This can lead to the detection of unexpected processes which might still be highly relevant. This is not only of technological, but also of fundamental relevance, as will be illustrated using the interaction of hydrogen with precovered surfaces as an example. Furthermore, the technologically and environmentally important interaction of oxygen with platinum surfaces will also be addressed.

2 Motivation

The interaction of molecules with surfaces is of high technological relevance. All materials interact with their environment through their surfaces. Sometimes this interaction can be harmful and lead, e.g., to corrosion or wear. However, also beneficial processes occur at

surfaces. Many chemical reactions are considerably facilitated at catalytic surfaces. This is of particular interest considering the importance of (electro-)chemical energy storage and conversion for the future energy technology. In order to improve the chemical activity of catalysts, it is important to understand how reactions proceed on surfaces. For decades, surface science studies, both experimental and theoretical, have been extremely successful in elucidating atomistic structures and processes on well-defined clean surfaces. Yet, many technologically relevant processes occur on precovered, structured surfaces. Therefore it is crucial to take into account the full complexity when studying such processes on surfaces.

3 Computational Method

The AIMD simulations have been performed using the periodic Vienna *Ab initio* Simulation Package (VASP)⁵ within the supercell approach. Electronic exchange and correlation have been described within the generalized gradient approximation (GGA)^{10,11}. The ionic cores have been represented either by ultrasoft pseudopotentials^{12,13} or by projected augmented wave (PAW) potentials^{14,15}. The convergence of the electronic structure calculations with respect to the energy cutoff representing the size of the plane-wave basis set and the \mathbf{k} -point sampling for the integration over the first Brillouin zone was carefully tested.

The AIMD simulations were performed using the Verlet algorithm¹⁶ with a time step of 1 fs within the microcanonical ensemble, i.e., the total energy was conserved during the simulations. This energy conservation was typically fulfilled to within ± 5 meV along a AIMD run. Sticking probabilities for each considered structure and incident kinetic energy were evaluated by averaging over 100 to 150 trajectories which were started with random initial lateral positions and orientations of the impinging molecules far enough above the surface. The statistical error of the sticking probabilities amounts to $\sigma = \sqrt{S(1-S)}/\sqrt{N}$ where S is the sticking probability and N the number of trajectories¹⁷. For $N \geq 150$, the statistical error is $\sigma \leq 0.04$, and for $N \geq 100$, $\sigma \leq 0.05$. Note that the statistical error does not depend on the complexity of the system, i.e., on the number of considered dynamical degrees of freedom, but only on the number of calculated trajectories.

4 Hydrogen adsorption on H-precovered Pd(100)

The adsorption of H₂ on Pd(100) represents one of the model systems in surface science for the study of adsorption phenomena. In addition to its importance in hydrogenation reaction this system is also interesting because of the fact that palladium can absorb huge amounts of hydrogen¹⁸. Because of the high sticking probability of H₂ on Pd(100)¹⁹, the surface becomes quickly covered by hydrogen once it is exposed to a H₂ gas. In order to model the adsorption of H₂ on H-precovered Pd(100), we have used (2×2) , (4×2) , (3×2) , and (3×3) unit cells with various amounts or preadsorbed hydrogen atoms. Note that there are typically several different arrangements of the adsorbed hydrogen atoms for a given coverage unless the surface is fully covered.

The results of more than 6,000 AIMD trajectory calculations with respect to the sticking probability at various hydrogen coverages are summarized in Fig. 1 where the sticking probability of H₂ on H-precovered Pd(100) is plotted as a function of the coverage. The different values of the sticking probability for the same hydrogen coverage are due to the

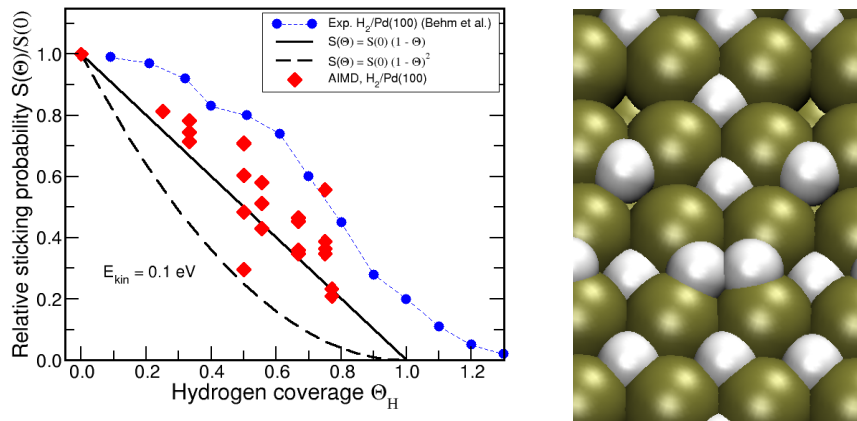


Figure 1. Relative dissociative adsorption probability $S(\Theta)/S(0)$ of hydrogen on hydrogen-covered Pd(100) as a function of coverage. The theoretical results are obtained for an initial kinetic energy of 0.1 eV at different configurations of the adsorbed hydrogen atoms whereas the experimental results by Behm *et al.*²⁰ are measured using a H_2 gas. In addition, a snapshot of an AIMD trajectory is shown for a hydrogen precoverage of $\Theta_H = 3/4$ in a 2×4 structure.

fact that several arrangements of the pre-adsorbed hydrogen atoms were considered which in general exhibit different sticking probabilities. In addition, the solid and the dashed line in Fig. 1 correspond to the sticking probability in the case of pure site-blocking without any dynamical effects if just one or two empty sites, respectively, are required for the H_2 adsorption. The fact that the AIMD sticking probabilities are larger than the results for pure site-blocking indicates that there are important dynamical effects such as steering or dynamical trapping in the adsorption process which enhance the sticking probability.

Experimental results²⁰ are also included in Fig. 1. Note that the calculations have been done for a mono-energetic molecular beam with a initial kinetic energy of $E_{kin} = 0.1 \text{ eV}$ whereas the experiment was performed with a H_2 gas. Still it is satisfying that the theoretical results trail the experimental ones.

In addition, in Fig. 1 two curves $S(\Theta) = S(0)(1 - \Theta)$ and $S(\Theta) = S(0)(1 - \Theta)^2$ are included which correspond to the sticking probability at a precovered surface if it is governed by pure site-blocking requiring one or two empty adsorption sites, respectively. The measured and most of the calculated sticking probabilities are above these two curves indicating that there are steering and trapping effects that lead to a higher sticking probability than expected for pure site-blocking although there is some slight repulsive interaction between pre-adsorbed hydrogen atoms and the impinging hydrogen molecule, as DFT calculations show. Interestingly enough, for the adsorption of H_2 on hydrogen-precovered Pd(111) both experimental and theoretical results find a dependence of the sticking probability on the coverage which is close to the $S(\Theta) = S(0)(1 - \Theta)^2$ curve²¹.

This significant difference between Pd(100) and Pd(111) is related to the fact that on Pd(100) the hydrogen atoms in the four-fold hollow adsorption site are located almost at the same height as the surrounding Pd atoms whereas on Pd(111) the adsorbed hydrogen atoms in the smaller three-fold hollow sites are positioned higher above the Pd atoms.

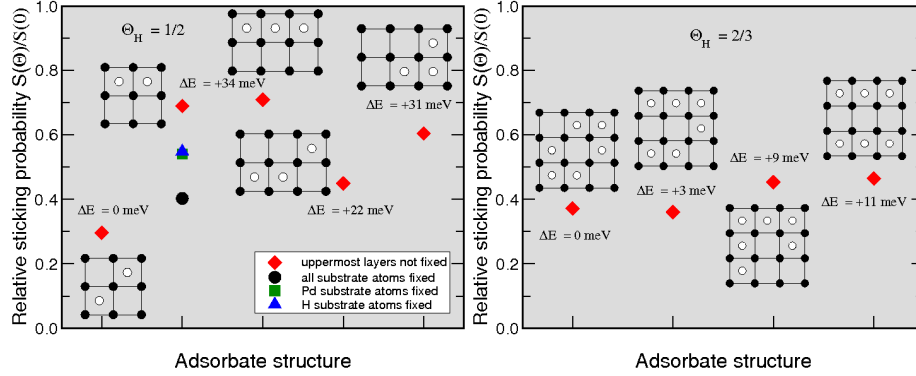


Figure 2. Calculated relative dissociative adsorption probability $S(\Theta)/S(0)$ of H_2 impinging on hydrogen-covered Pd(100) with a coverage of $\Theta_H = 1/2$ and $\Theta_H = 2/3$, respectively, with an initial kinetic energy of $E_{\text{kin}} = 0.1$ eV for three different adsorbate structure within a (3×3) periodicity as indicated in the insets. In addition, the stability ΔE in meV of the adsorbate structures per hydrogen atom with respect to the most favorable structure is given in the figure.

Consequently, on Pd(100) the adsorbed hydrogen atoms are effectively shielded by the Pd atoms leading to a rather small mutual repulsion between the hydrogen atoms. On Pd(111), there is a stronger H-H repulsion which effectively leads to the much lower sticking probability than on Pd(100) at the same hydrogen coverage.

The fact that there is still some admittedly small mutual hydrogen repulsion on Pd(100) is illustrated in Fig. 2 where for several hydrogen adsorbate structures their stability ΔE per hydrogen atom with respect to the most favorable structure is given. Typically, the more compact the H-adsorbate structures, i.e., the higher the number of nearest-neighbor H atoms, the less stable the structure is. For the corresponding sticking probability of H_2 molecules impinging on these particular structures that is also plotted in Fig. 2, we find an anti-correlation with respect to the stability. The more compact H structures which as a consequence also exhibit compact vacancy structures lead to higher sticking probabilities. Still, it is important to realize that also on substrates where there is no dimer vacancy present, as for the most stable structures included in Fig. 2, still H_2 dissociative adsorption is possible. The dissociation starts with one H atom entering the four-fold hollow site with the other H atom remaining at a neighboring bridge site. From there, it propagates in an exchange-like mechanism until it finds an empty hollow site.

For one particular $\Theta_H = 1/2$ structure within a 2×2 geometry, simulations with different subsets of substrate atoms kept fixed have been performed. The corresponding sticking probabilities also plotted in Fig. 2 show that there is a strong dependence of the sticking probability on the recoil of the substrate atoms, much stronger than on flat surfaces⁷. This again indicates the importance of dynamical effects in these strongly corrugated, non-activated system.

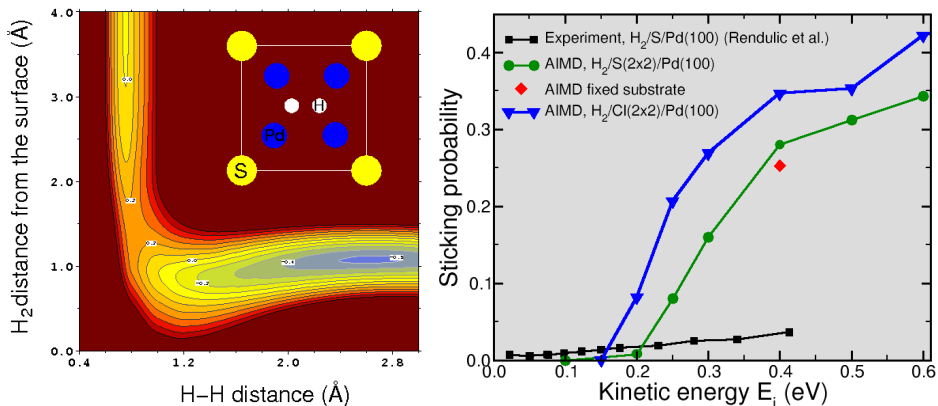


Figure 3. Left panel: Two-dimensional cut through the potential energy surface of $\text{H}_2/\text{S}(2 \times 2)/\text{Pd}(100)$ as a function of the H-H distance and the H_2 distance from the surface calculated by periodic DFT calculations. The inset illustrates the molecular orientation and lateral center of mass position. The contour spacing is 0.1 eV. Right panel: Sticking probability determined in AIMD simulations for H_2 impinging on $\text{S}(2 \times 2)$ - and $\text{Cl}(2 \times 2)$ -covered $\text{Pd}(100)$. For $E_{\text{kin}} = 0.4$ eV and $\text{H}_2/\text{S}(2 \times 2)/\text{Pd}(100)$, the AIMD result for a fixed substrate is also shown. In addition, the measured sticking probability of H_2 on S-covered $\text{Pd}(100)$ ¹⁹ is included.

5 Hydrogen adsorption on S- and Cl-precovered Pd(100)

Both the study of sulfur as well as chlorine co-adsorption is technologically relevant and interesting. Sulfur is known as a poison for the car exhaust catalyst, and on $\text{Pd}(100)$, it leads to a significant reduction of the hydrogen dissociation probability^{19,22}. The specific adsorption of chlorine is a typical process occurring at electrochemical metal-electrolyte interfaces. Whereas there is already some mutual repulsion between adsorbed hydrogen atoms, preadsorbed sulfur or chlorine atoms lead to much stronger repulsion, turning the non-activated H_2 adsorption on $\text{Pd}(100)$ into an activated none, i.e., there are no longer any paths without any barrier towards dissociative adsorption²³.

The minimum barrier for H_2 dissociation on $\text{S}(2 \times 2)/\text{Pd}(100)$ is illustrated Fig. 3 where a two-dimensional cut through the potential energy surface is shown. Whereas the particular path shown in Fig. 3 is non-activated on clean $\text{Pd}(100)$ ²⁴, it becomes hindered by a barrier of about 0.25 eV. In fact, chlorine adsorption has a rather similar effect as sulfur on the H_2 - $\text{Pd}(100)$ interaction, the barriers are just 50 meV smaller.

Such a poisoning of the substrate of course also changes the adsorption dynamics significantly from non-activated to activated behavior, i.e., the sticking probability typically increases monotonically with the incident kinetic energy, as Fig. 3 shows, where the results of AIMD simulations are also shown. The difference in the minimum barrier heights between $\text{H}_2/\text{S}(2 \times 2)/\text{Pd}(100)$ and $\text{H}_2/\text{Cl}(2 \times 2)/\text{Pd}(100)$ are reflected in the corresponding shift between the sticking curves. Interestingly, keeping the substrate fixed modifies the sticking probability only to a small extent. Apparently for an activated system the recoil of the substrate atoms matters less than for a strongly corrugated non-activated system (see Fig. 2).

Still, for $\text{H}_2/\text{S}(2 \times 2)/\text{Pd}(100)$ there is a large discrepancy between AIMD and exper-

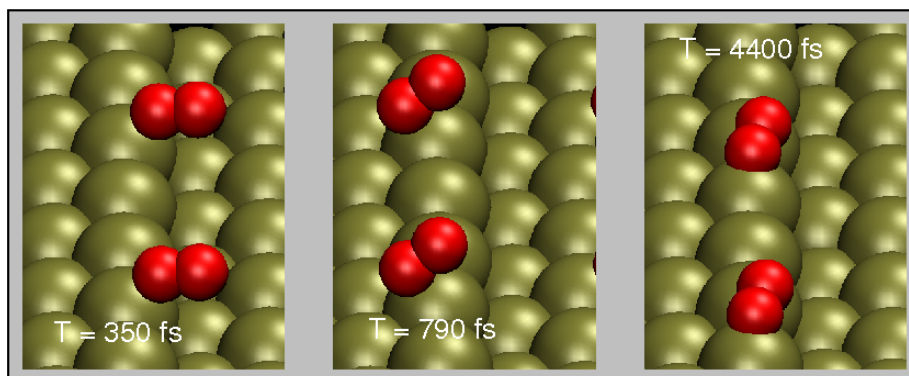


Figure 4. Snapshots of an AIMD trajectory of O_2 impinging on Pt(211) with an initial kinetic energy of $E_{kin} = 0.1$ eV.

imental results. Although short-comings of DFT calculations can never be excluded, it should be noted that experimentally the preparation of an ordered (2×2) sulfur overlayer on Pd(100) has not been fully confirmed^{19,25}. Hence the discrepancy might be due to different sulfur overlayers realized in the calculations and in the experiment.

6 Interaction dynamics of O_2 with stepped Pt

The adsorption of O_2 on Pt is one of the crucial steps occurring in the car exhaust catalyst. Since realistic catalysts do not correspond to low-index single crystal surfaces but rather consists of small particles with high step densities, it is important to clarify the role of steps in catalytically important reactions. On Pt(111), direct O_2 dissociation does not occur due to steric hindrance^{26,27}, but it is still unclear whether it might happen at stepped surfaces where the energy gain upon adsorption is much larger²⁸.

From a technical point of view, DFT simulations including O_2 are much more demanding than simulations involving H_2 due to the fact that O_2 is in the triplet state in the gas phase which requires a spin-polarized treatment. This does not only mean that twice as many basis functions have to be taken into account for both the spin up and the spin down components, but typically the convergence of the self-consistent field iteration to solve the Kohn-Sham equations is much worse compared to spin-unpolarized calculations.

Still, it is possible to run AIMD trajectories in the O_2 /Pt(211) system. First preliminary results are shown in Fig. 4 where snapshots of a trajectory of O_2 impinging on Pt(211) are depicted. After 350 fs, the O_2 molecules hits the surface with one atom above the lower side of the step. Still, the O_2 molecule is steered towards the upper side of the step ($T = 790$ fs) where the most favorable adsorption site is located. Here, the molecule becomes molecularly trapped in the most favorable molecular adsorption site ($T = 4.4$ ps) that has already been identified in DFT calculations²⁸.

The AIMD simulations thus indicate that indeed steps do attract impinging O_2 molecules. Still, so far no dissociative adsorption event has been observed for O_2 /Pt(211). Therefore it remains to be seen whether O_2 dissociation on Pt(211) is a two-step process as on Pt(111)²⁷ or whether it rather corresponds to a direct event.

7 Concluding Remarks

This study has illustrated that ab initio molecular dynamics studies are a powerful tool to study the adsorption of molecules on complex surface structures, such as precovered or stepped surfaces. The unbiased nature of the AIMD simulations allows important insights into the reaction dynamics on surfaces as long as several hundred trajectories are sufficient to obtain statistically meaningful results. Since the statistical error of the AIMD simulations with respect to the sticking probability does not depend on the complexity of the considered systems, AIMD simulations are also well-suited to address the adsorption dynamics of larger molecules such as e.g. small organic molecules. Simulations along these lines are planned for the future.

Acknowledgments

Many fruitful discussions with Fabio Busnengo and Ariel Lozano are gratefully acknowledged. The simulations presented in this work were made possible by a grant of computer time provided by the NIC of the Research Centre Jülich.

References

1. D. Marx and J. Hutter, Ab initio Molecular Dynamics: Theory and Implementation, in *Modern Methods and Algorithms of Quantum Chemistry*, edited by J. Grotendorst, volume 3 of *NIC series*, pages 329–477, John von Neumann-Institute for Computing, Jülich, 2000.
2. S. Lorenz, M. Scheffler, and A. Groß, Descriptions of surface chemical reactions using a neural network representation, *Phys. Rev. B* **73**, 115431 (2006).
3. A. Groß, M. Bockstedte, and M. Scheffler, Ab initio molecular dynamics study of the desorption of D₂ from Si(100), *Phys. Rev. Lett.* **79**, 701 (1997).
4. L. C. Ciacchi and M. C. Payne, "Hot-Atom" O₂ Dissociation and Oxide Nucleation on Al(111), *Phys. Rev. Lett.* **92**, 176104 (2004).
5. G. Kresse and J. Furthmüller, Efficient iterative schemes for ab initio total-energy calculations using a plane-wave basis set, *Phys. Rev. B* **54**, 11169 (1996).
6. B. Hammer, L. B. Hansen, and J. K. Nørskov, Improved adsorption energetics within density-functional theory using revised Perdew-Burke-Ernzerhof functionals, *Phys. Rev. B* **59**, 7413 (1999).
7. A. Groß and A. Dianat, Hydrogen dissociation dynamics on precovered Pd surfaces: Langmuir is still right, *Phys. Rev. Lett.* **98**, 206107 (2007).
8. A. Groß, Ab initio molecular dynamics study of hot atom dynamics after dissociative adsorption of H₂ on Pd(100), *Phys. Rev. Lett.* **103**, 246101 (2009).
9. A. Groß, Ab initio molecular dynamics simulations of the adsorption of H₂ on palladium surfaces, *ChemPhysChem* **11**, 1374 (2010).
10. J. P. Perdew, J. A. Chevary, S. H. Vosko, K. A. Jackson, M. R. Pederson, D. J. Singh, and C. Fiolhais, Atoms, molecules, solids, and surfaces: Applications of the generalized gradient approximation for exchange and correlation, *Phys. Rev. B* **46**, 6671 (1992).

11. J. P. Perdew, K. Burke, and M. Ernzerhof, Generalized gradient approximation made simple, *Phys. Rev. Lett.* **77**, 3865 (1996).
12. D. Vanderbilt, Soft self-consistent pseudopotentials in a generalized eigenvalue formalism, *Phys. Rev. B* **41**, 7892 (1990).
13. G. Kresse and J. Hafner, Norm-conserving and ultrasoft pseudopotentials for the first-row and transition elements, *J. Phys.: Condens. Matter* **6**, 8245 (1994).
14. P. E. Blöchl, Projector augmented-wave method, *Phys. Rev. B* **50**, 17953 (1994).
15. G. Kresse and D. Joubert, From ultrasoft pseudopotentials to the projector augmented-wave method, *Phys. Rev. B* **59**, 1758 (1999).
16. L. Verlet, Computer "experiments" on classical fluids. I. Thermodynamical properties of Lennard-Jones molecules, *Phys. Rev.* **159**, 98 (1967).
17. P. M. Agrawal, A. N. A. Samadh, L. M. Raff, M. T. Hagan, S. T. Bukkapatnam, and R. Komanduri, Prediction of molecular-dynamics simulation results using feed-forward neural networks: Reaction of a C₂ dimer with an activated diamond(100) surface, *J. Chem. Phys.* **123**, 224711 (2005).
18. A. Pundt and R. Kirchheim, Hydrogen in metals: Microstructural aspects, *Annu. Rev. Mater. Res.* **36**, 555–608 (2006).
19. K. D. Rendulic, G. Anger, and A. Winkler, Wide range nozzle beam adsorption data for the systems H₂/nickel and H₂/Pd(100), *Surf. Sci.* **208**, 404 (1989).
20. R. J. Behm, K. Christmann, G. Ertl, and M. A. Van Hove, Adsorption of CO on Pd(100), *J. Chem. Phys.* **73**, 2984 (1980).
21. Y. Xiao and W. Dong, Molecular dynamics simulation of a complex surface reaction: The effect of coverage on H₂ dissociation on Pd(111), *Phys. Rev. B* **83**, 125418 (2011).
22. M. L. Burke and R. J. Madix, Hydrogen on Pd(100)-S: The effect of sulfur on precursor mediated adsorption and desorption, *Surf. Sci.* **237**, 1 (1990).
23. C. M. Wei, A. Groß, and M. Scheffler, Ab initio calculation of the potential energy surface for the dissociation of H₂ on the sulfur-covered Pd(100) surface, *Phys. Rev. B* **57**, 15572 (1998).
24. S. Wilke and M. Scheffler, Potential-energy surface for H₂ dissociation over Pd(100), *Phys. Rev. B* **53**, 4926 (1996).
25. M. Rutkowski, D. Wetzig, H. Zacharias, and A. Groß, Rotational and vibrational population of D₂ desorbing from sulfur-covered Pd(100), *Phys. Rev. B* **66**, 115405 (2002).
26. C. T. Rettner and C. B. Mullins, Dynamics of the chemisorption of O₂ on Pt(111): dissociation via direct population of a molecularly chemisorbed precursor at high-incidence kinetic-energy, *J. Chem. Phys.* **94**, 1626 (1991).
27. A. Groß, A. Eichler, J. Hafner, M. J. Mehl, and D. A. Papaconstantopoulos, *Ab initio* based tight-binding molecular dynamics simulation of the sticking and scattering of O₂/Pt(111), *J. Chem. Phys.* **124**, 174713 (2006).
28. P. Gambardella, Ž. Šljivančanin, B. Hammer, M. Blanc, K. Kuhnke, and K. Kern, Oxygen dissociation at Pt steps, *Phys. Rev. Lett.* **87**, 056103 (2001).